

Impact of Aviation Electrification on Airports: Flight Scheduling and Charging

Boya Hou

Subhonmesh Bose

Lavanya Marla

Kiruba Haran

Abstract—Electrification can help to reduce the carbon footprint of aviation. The transition away from the jet fuel-powered conventional airplane towards battery-powered electrified aircraft will impose extra charging requirements on airports. In this paper, we first quantify the increase in energy demands at several airports across the United States (US), when commercial airline carriers partially deploy hybrid electric aircraft (HEA). We then illustrate that smart charging and minor modifications to flight schedules can substantially reduce peak power demands, and in turn the needs for grid infrastructure upgrade. Motivated by our data analysis, we then formulate an optimization problem for flight rescheduling that incorporates HEA charging considerations. This problem jointly decides flight schedules and charging profiles to manage airport congestion and peak power demands. We further consider mechanisms via which airlines and airports can negotiate HEA assignments using said optimization problem. Finally, we illustrate the efficacy of our formulation through a case study on the John F. Kennedy International Airport.

I. INTRODUCTION

Commercial aviation produced 915 million tonnes of CO₂ worldwide in 2019, responsible for 2% of all human-induced CO₂ emissions from energy consumption, as per [1]. The carbon footprint of aviation is projected to increase with predicted annual growth of 4.2% in demand for air travel over 2018-2038, according to [2], with temporary reductions due to COVID-19, per [3]. The corresponding increase in greenhouse gas emissions will pose a serious threat to the vision of a carbon-neutral future. Electrification has been identified as a potential path to reduce said emissions, e.g., by [4], [5].

Electrified aircraft are an emergent technology, largely enabled by the development efforts supported by NASA's Advanced Air Transport Technologies program in the United States and similar programs by the respective agencies in the European Union and Asia. Various aircraft configurations such as turbo-electric, hybrid-electric and all-electric have been proposed and analyzed. By hybrid electric configuration, we mean those airplanes which are propelled partly by electric motor through a battery system and partly by gas turbines through jet fuel. The benefits of a parallel hybrid propulsion system for boosting power during takeoff and climb has been demonstrated in [6] and [7]. Flight performance of parallel turbofan systems has been analyzed in [8]. Small electric airplanes for general aviation are already available. Flight demonstrations are underway for the commuter class with planes carrying <20 passengers. The next step is to electrify

regional airplanes that accommodate 30 - 100 passengers. Various studies such as those in [9], [10] predict that commercial aviation will adopt electric aircraft over the next few decades (in the 2030-2050 time-frame).

To handle the impending electrification of commercial aviation, airports must invest in appropriate charging infrastructure, as emphasized very recently in the World Economic Forum [5]. Investment into building such infrastructure must be forward-looking and account for plausible growth trajectories of electrification technology. We first gauge the energy and power needs of hybrid electric aircraft (HEA) at major airports across the United States (US), accounting for the schedules of various airlines at the airport. We only consider those HEA configurations that are deemed to become viable over the 2030-2050 time frame, according to academic and industrial research. Scheduling of flights at an airport is intimately related to when and how much the electrified aircraft operating these flights can be charged. As we demonstrate, one substantially impacts the other. The main focus of this paper is to show that fleeting decisions of airlines with electric aircraft cannot be done independently of other airlines' decisions, and are inextricably linked to their scheduling decisions. The formulation and analysis of flight rescheduling protocols must be solved *across* airlines that operate at an airport whose capacitated grid infrastructure constrains HEA charging. Towards this goal, we jointly aim to optimize flight arrivals/departures and decide the charging profiles of HEA at an airport, aiming to minimize airport congestion and peak electric power demands from HEA. To do so, we tally the pros and cons of two possible mechanisms for congestion management. The first mechanism allows a central authority such as the airport to centrally solve the rescheduling problem. The second one designs a negotiation strategy, where airlines propose schedules and the airport runs the rescheduling problem as a feasibility check, and the cycle continues till all parties agree. In this paper, we restrict our congestion management interventions to rescheduling protocols at airports at the strategic or planning phase, which account for airport-wide constraints on movements and charging. Similar questions can be studied for tactical or real-time operations; such investigations are relegated to future work.

Not all flights can be operated using HEA. Energy densities of today's batteries are in the 200-250 Wh/kg range. They are substantially smaller than that of jet fuel with densities of ~13,000 Wh/kg. As a result, the size and the weight of a battery required on board limits the range of an HEA. The battery size also depends on the extent the aircraft relies on electric propulsion as opposed to jet fuel. With plausible configurations

All authors are affiliated with the University of Illinois at Urbana-Champaign, IL 61801. B. Hou, S. Bose, and K. Haran are with the Department of Electrical and Computer Engineering, and L. Marla is with the Industrial and Enterprise Systems Engineering. Emails: {boyahou2, bores, lavanyam, kharan}@illinois.edu

of battery energy densities and degree of hybridization, we compute the energy needs for operating HEA on domestic flight paths within continental US in Section II. By switching flights from current schedules that can be operated by HEA, we estimate the increase in annual energy needs at various US airports. Our estimates indicate that accommodating HEA in commercial aviation will require substantial upgrades to the grid infrastructure that powers these airports. This estimation, albeit simplistic, motivates us to examine the joint questions of flight scheduling and charging at airports with HEA.

While flight distance, number of passengers and airplane type largely dictate the energy needs for HEA, *peak power* requirements from the grid on the other hand, depend on the *rate* of charging. Grid components, such as transformers, must be sized properly to support such peak rates. In Section III, we show that reflecting by converting feasible aircraft to HEA without modifying schedules, and charging such HEA at constant power levels over their dwell times at airports, can lead to substantial peak power demands. Thus, optimizing charging schedules can significantly lower these peaks at airports.

Flight arrival and departure schedules define the dwell times of flights at airports. For HEA, these schedules put constraints on when and how much an airplane can be charged. Thus, not surprisingly, alterations in schedules of some flights can further shrink peak power requirements over and above that obtained from optimizing charging schedules alone. Our results in Section III indeed align with this expectation. Charging considerations alone cannot define flight schedules, however. Airlines tailor their requests for flight arrivals and departures to suit passenger demand patterns. As a result, busy airports often witness congestion during peak hours. Congestion leads to flight delays at these airports. Such delays for multi-hop flight paths tend to cascade across airports. Flight rescheduling for congestion management has been widely studied, e.g., see [11] for a survey. Airports in the European Union and level 3 airports in the US (e.g., John F. Kennedy International Airport (JFK), LaGuardia Airport (LGA), and Ronald Reagan Washington National Airport (DCA)) adopt such mechanisms for congestion management, according to [12]. Along the same lines, we formulate a flight rescheduling problem at an airport that accounts for charging considerations of HEA in Section IV. Specifically, we design an optimization model that seeks to jointly minimize the displacements of flights from their requested schedules by airlines and flatten the power profile required to charge the HEA aircraft operating these schedules.

Many American airports today do not impose congestion management protocols. This suggests that one can operate airports without such protocols, albeit with increased and frequent travel delays. The introduction of HEA into airline fleet will likely change that paradigm. Installed capacities of charging infrastructure at airports impose *hard constraints* on charging decisions. In general, one cannot frequently exceed grid equipment limitations, without seriously damaging said equipment. We emphasize that this limitation does not arise solely due to the lack of energy availability. Rather, the installed sizes of transformers and electric power lines for the grid dictate the maximum rate at which energy can be

delivered. Thus, feasibility of charging schedules must be checked *across* airlines at an airport. In Section IV, we propose two congestion management techniques, building on the rescheduling algorithm with HEA charging considerations. In the first protocol, the airport centrally solves the flight rescheduling and charging problem, and suggests which flight paths should switch HEA with conventional aircraft to ensure acceptable schedule adjustments. In the other, an iterative process ensues, where the airport runs the rescheduling algorithm, but asks each airline to submit a revised schedule, and the process continues till schedule readjustments are acceptable to the airlines and are operationally feasible at the airport. We remark that these are only two among possible mechanisms for readjustment of schedules with HEA. A more detailed analysis must account for possible re-submissions of scheduling requests from airlines and reassignments of flight paths between HEA and conventional aircraft, with possible dynamic reassignments for tactical operations; and consideration of inter-airline equity and other multiple criteria. We leave such investigations for future endeavors.

We run a representative case study of the joint rescheduling and charging algorithm with HEA charging for the John F. Kennedy International Airport (JFK) in Section V. Our experiments reveal the importance of jointly considering flight rescheduling and smart HEA charging with reasonable HEA adoption via reflecting. In particular, we solve the flight rescheduling problem *without* HEA charging considerations and then construct charging profiles for HEA under a constant power charging scheme. Such a construction results in a high peak power demand of 35.9 MW. Enforcing a limit of 20 MW on power drawn for charging, our optimization problem returns a solution that reduces that peak to 14.6 MW with a different flight schedule. Using our simulation framework, we also study how declared capacities at the airport and charging constraints on airplane batteries impact both flight schedules and charging profiles. By declared capacity, we mean the quantified measure of the ability of an airport to support a certain number of flight movements within a time duration, that may reflect capacities of runways, terminals/gates, ground-crew, etc. The results illustrate that airport congestion and charging considerations are inter-dependent and cannot be tackled separately. We finally compare the two congestion management protocols. Our results illustrate that more flight paths operate HEA when the airport suggests which HEA route should switch to conventional aircraft, rather than when airlines themselves revise their proposed routes operated by HEA and iterate with airport's feasibility check. In other words, given the coupling between charging and scheduling considerations, centralized joint airport and grid congestion management might play a key role in HEA operation—and over the long run—adoption.

We draw on two lines of relevant work—one that characterizes the capabilities and impacts of electric airplanes, and the other that studies flight rescheduling and de-peaking algorithms. In the first line of research, the most relevant works are those of [10], [13] that quantify the capabilities of HEA concepts. We focus on retrofitted regional and single-aisle HEA configurations in Table I that academic and industry research deem viable over the next few decades. Leveraging

the technology growth scenarios envisioned in these works, we examine the impacts of HEA adoption on airport operations, and provide a granular view of the impact of HEA on electric power demands, not just at a global scale as done in [9], but at the level of airports. In the second category, there is a growing

TABLE I: Summary of regional and single-aisle hybrid electric aircraft concepts and research. BSED stands for battery specific energy density.

Research group	BSED (Wh/kg)	Reference
Boeing-GE SUGAR Volt	750	[14], [15]
Bauhaus	1000-1500	[16]
UTRC	Not spec.	[4]
Airbus	800	[17]
Cambridge	750	[18]
Georgia Tech	750	[4]

literature on flight scheduling at capacity-constrained airports. See [11], [19]–[26] among others. These papers optimize flight schedules to limit congestion during peak hours at airports to avoid flight delays, the total cost of which in the US has been estimated to be \$33 billion by the [27]. We build on these models to jointly optimize schedules of all flights and the charging profiles of HEA at capacity-constrained airports. Indeed, our case study on JFK airport indicates how one cannot disentangle these two problems once HEA are introduced into airlines’ schedules. In a sense, we introduce a widely studied question for electrified ground vehicles to the domain of electrified aviation—smart charging for peak demand reduction. Benefits of said reduction are well-studied, e.g., in [28]–[31], that include deferring infrastructure upgrades of electric power distribution/transmission networks and avoiding peak demand charges. Given the scale of HEA energy and power needs, we believe that smart charging of HEA will become similarly important, and alleviate burdens on airport infrastructure growth, as outlined in [5].

II. ESTIMATING ENERGY REQUIREMENTS OF HEA

Energy needs of operating a flight path or an aircraft route with HEA will depend on the the type of aircraft being electrified and the distances traveled. For flight paths, we focus on short-haul domestic commercial flights that had a dwell time longer than 15 minutes at the originating airport in 2018. We use flight information from the airline on-time performance data from the [32]. The range of an HEA is limited by the size and weight of the battery on-board. Battery technology for electric airplanes is constantly improving. These batteries are characterized by two parameters—its battery specific energy density (BSED) and its motor factor (MF). BSED, measured in Wh/kg, dictates the weight of the battery required to deliver a given amount of electrical energy. And, MF defines the ratio of the peak power that can be delivered by the battery and that required by the aircraft. For a specific BSED-MF combination, we utilize the range capabilities of retrofit hybrid electric regional jets and narrow body aircraft from [10], reproduced in Appendix Table II. A specific flight can utilize HEA only if the flight distance is within this range.

We now formally describe the electrical energy requirement of operating an aircraft’s route or path with HEA. Assume that

each HEA arrives at an airport with a depleted battery and needs to be charged up to the level required for its next flight. The required energy is calculated as $E = p \times d \times b_0$, where d describes the next flight distance in miles, p is the number of passengers and b_0 denotes the battery energy usage per passenger-mile¹. This calculation assumes that the electrical power drawn from the battery remains roughly constant during different phases of the flight, e.g. taxi, take-off and landing. For each flight in the database from the [32], we use the tail number to identify the aircraft type from airplane manufacturer’s websites; which in turn, yields the total number of seats on the plane. Throughout this analysis, we uniformly assume that 85% of all seats are filled in each flight to estimate p . This load factor matches the yearly average estimates of the same in the industry, based on the [33]. The values of parameter b_0 for HEA are adopted from [10], reproduced in Table I in the Appendix, assuming a battery-pack voltage of 128V. Sizing of such batteries accounts for battery energy consumed during taxi, takeoff, cruise, approach, and landing. For regional jets, we use b_0 for ERJ-175 and for single-aisle aircraft, we use that for Boeing 737-700.

To illustrate the calculations through an example, consider a single hybrid electric retrofit of Embraer ERJ 170-200 aircraft with tail number N178SY. On 05/29/2018, this aircraft operated a 599-mile flight from SFO (San Francisco International Airport, CA) to SLC (Salt Lake City, UT). N178SY arrived at SFO at 17:02 pm and left for SLC at 17:53 pm. For different MF and BSED configurations, Table II records E . For this example, a BSED of 500 Wh/kg and MF of 25% does not have the range ability to cover 599 miles. As a result, with this BSED-MF combination, N178SY cannot be operated with HEA.

TABLE II: Power requirements of aircraft N178SY for flight from SFO to SLC.

MF (%)	BSED (Wh/kg)	
	500	700
12.5	1.05 MWh	1.03 MWh
25	/	2.14 MWh

A. Annual Energy Requirements at US Airports

The energy demands for individual flights under BSED-MF combinations prove useful in later sections to both analyze and design charging schedules for HEA. In this study, we consider BSED and MF values that are deemed feasible in the 2030-2050 time-frame, according to [4], [14]–[17] and [18]. Here, we utilize our calculations to estimate the increase in annual energy demands at major US airports with plausible growth trajectories of HEA technology, with flight schedules from the BTS dataset for 2018. For a given BSED-MF, we deem a flight feasible to be switched to HEA if its flight distance is within the range of its retrofitted hybrid electric variant. This step defines the maximum size of the domestic

¹The energy use per passenger mile gives a first-order estimate of energy required for aircraft of different sizes (within a reasonable range) with close-to-average occupancy rates.

²For BSED ≤ 700 Wh/kg, MF $\geq 50\%$ is impractical for any flight distance.

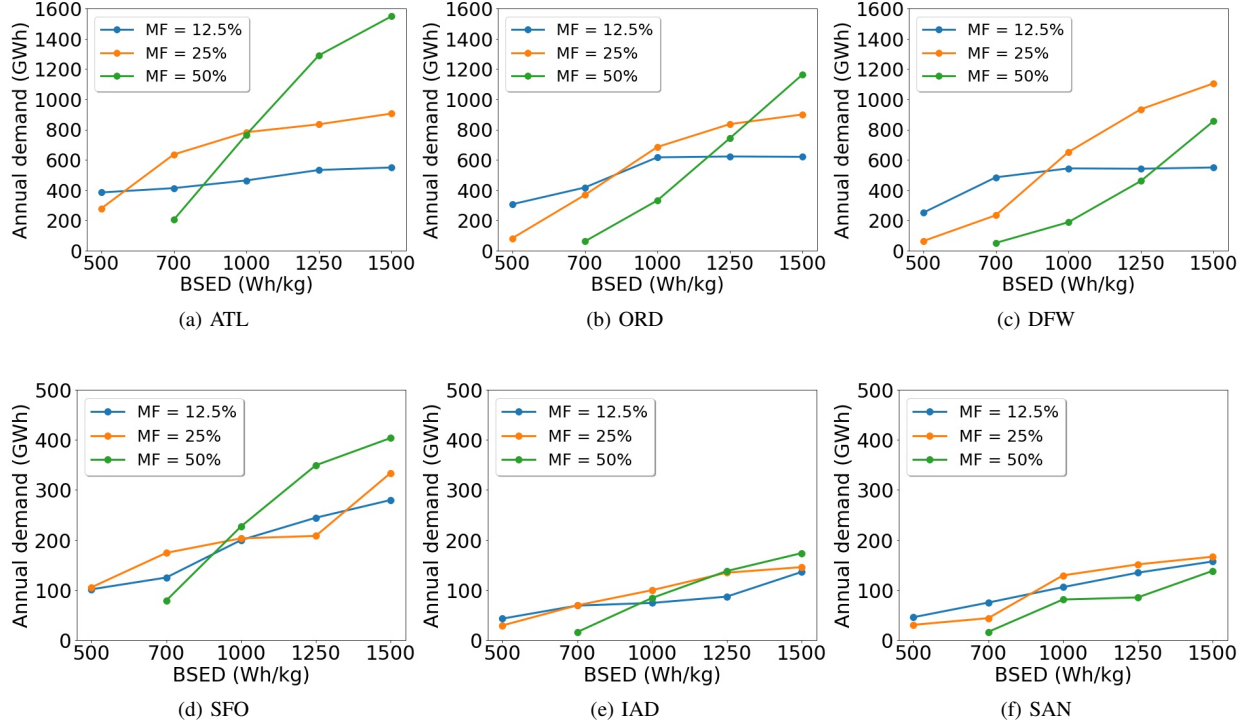


Fig. 1: Extra annual electricity demand that results from charging commercial passenger domestic HEA at airports across US under various BSSED-MF combinations.²

fleet that gets electrified. See A for the total number of flights that can be operated as HEA under various BSSED-MF combinations at the major US airports. We remark that our estimates are premised upon simplified assumptions of HEA operations and their energy requirements as discussed above, and operating parameters of HEA concepts from [10]. Despite being simplistic, our analysis provides an airport-level granular view into energy/power requirements than global estimates in [9] obtained with a single electric airplane concept adopted from [13]. We view this endeavor as an important step to motivate our investigation in the next section of jointly optimizing scheduling and charging decisions.

Figure 1 plots the projected increase in aggregate annual electricity demands at six large airports in the United States—Hartsfield-Jackson Atlanta International Airport (ATL), Chicago O’Hare International Airport (ORD), Dallas/Fort Worth International Airport (DFW), Dulles International Airport near Washington D.C. (IAD) and San Francisco International Airport (SFO). The plots reveal that even moderate BSSED and MF values for HEA will lead to a substantial annual battery energy consumption. To illustrate the magnitude of that increase, notice that aggregate energy demand of SFO in 2018 was 311 GWh, according to the DataSanFrancisco program. Figure 12d confirms that electrification at SFO with any BSSED-MF combination will substantially amplify said demand of 311 GWh. The phenomenon is similar for other airports. For example, ORD had an annual total energy demand of 441 GWh in 2002 according to the O’Hare Modernization Final Environmental Impact Statement. The projected increase in ORD will more than double that requirement even at BSSED

= 700 Wh/kg and MF = 25%. For the purposes of this initial analysis, we ignore the possibility that an HEA may need to charge enough to complete a round-trip journey from and to that airport if the destination airport lacks necessary charging infrastructure. Accounting for such possibilities will only increase our demand estimates.

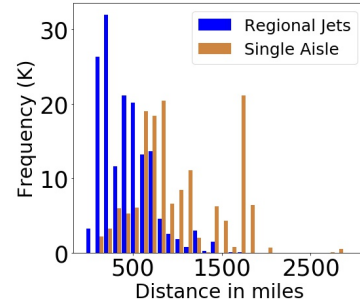


Fig. 2: Frequency of flight distances for regional jets and single aisle aircraft flying out of ORD in 2018.

For a given MF, one might expect total energy consumption from batteries on HEA to decrease with BSSED, because one requires lighter batteries to deliver the same amount of power. However, that is not always the trend in Figure 1. To explain this apparent paradox, we plot the histograms of flight distances in Figure 2 served by regional jets and single aisle aircraft at ORD in 2018. Notice that the distance distribution of single-aisle aircraft is more right-skewed than that of regional jets. Higher BSSED values allow larger travel distances. As a result, more single-aisle aircraft, traveling longer distances with higher energy needs, are converted to hybrid. Consequently,

energy needs of HEA increase. In Figure 3, we illustrate this further by breaking down the energy requirement into two components. We begin by considering the set of flights operated via HEA at BSED = 500 Wh/kg and MF = 25%. The black line measures the energy requirements of the same flight paths as BSED varies between 500 Wh/kg and 1500 Wh/kg with the same MF. Thanks to improvements in battery technology at higher BSED values, less electric energy is required to operate the same flight trips, reducing the baseline energy requirements that define the first component. However, the total energy requirements (plotted in red) increases as higher BSED values allow larger travel distances, making way for more long-distance flights with higher energy needs served by HEA. The longer travel distances contribute to the second component of the energy requirement, which increases faster than the reduction in the first component with BSED.

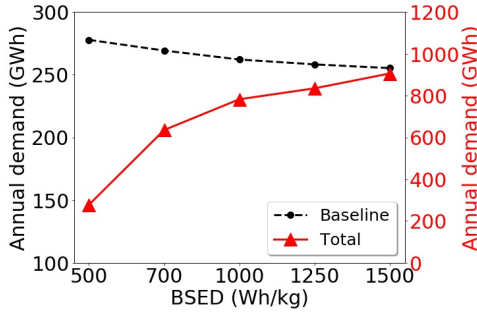


Fig. 3: Breakdown of the energy requirement as BSED increases. The baseline captures the energy requirements from the same set of flight paths that operate an HEA at BSED of 500 Wh/kg, but calculated at other values of BSED. The total energy draw measures the aggregate energy requirement from the aforementioned flight paths and others that become viable at higher BSED values.

III. PEAK POWER REQUIREMENTS AND PEAK SHAVING MECHANISMS

Grid infrastructure to deliver power at airports must be designed to cover daily peak power demands from HEA and the rest of the airport. In this section, we study the peak power requirements for HEA charging at various airports.

Consider a naive charging scheme, where the energy requirement of HEA is delivered uniformly at constant power over its dwell-time at the airport. This power, summed across all airplanes at each time yields the power requirement of HEA at the airport. In Figure 4, we plot the histograms of daily peak powers from HEA charging at SFO using the BTS dataset for 2018 under different BSED settings with MF = 12.5%. With BSED of 500, 700 and 1000 Wh/kg, we obtain median peak power demands of 25.8, 33.7 and 54.7 MW, respectively. The daily maxima are even higher, e.g., with BSED of 1000 Wh/kg, the highest daily peak is ~82 MW. These demands are substantial, given that the average power demand of SFO in 2018 was 35 MW, according to the DataSanFrancisco program. Supporting grid infrastructure at the airports, including transformers and distribution lines, must be sized to handle the power requirements of HEA. Peak powers from naive charging will pose steep requirements on the grid infrastructure. Even if transformers are properly sized,

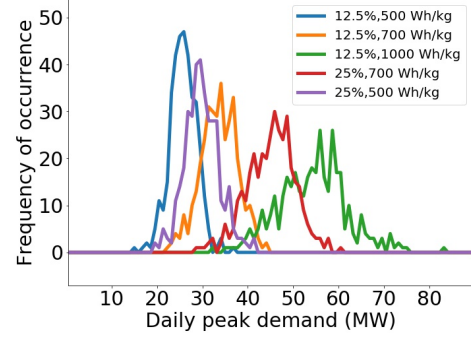


Fig. 4: Histogram of daily peak demands with different BSED (in Wh/kg) and MFs (in %) at SFO with flight schedule data from 2018.

large peak demands typically increase power procurement costs manifold. This nonlinearity in the growth of procurement costs with peak demand arises due to the fact that generators committed to supply these infrequent peaks have much higher production costs than those used to supply base load. Smart coordinated charging among HEA can shave daily peaks.

A. Shaving Peak Power Demands

We now illustrate the potential of smart charging at airports to reduce daily peak power demands at airports. Assume for this subsection that flight schedules remain the same, that is, the arrival and the departure times for each flight are the same as those in the [32] database. Divide the day into $T = 1440$ one-minute intervals. We consider the charging of HEA fleet \mathcal{F} , indexed by n . For aircraft n , let t_n^A and t_n^D , respectively, denote its arrival and departure times at the airport gate. Define E_n as its total energy needs for the next flight leg. With γ_n^t denoting the charging rate (power) drawn by HEA n in period t , we formulate the smart charging problem as

$$\begin{aligned} & \text{minimize} && \sum_{t=0}^{T-1} \left(\sum_{n \in \mathcal{F}} \gamma_n^t \right)^2, \\ & \text{subject to} && \sum_{t=0}^{T-1} \gamma_n^t \Delta t = E_n, \quad \gamma_n^t = 0 \text{ for } t \notin [t_n^A, t_n^D], \\ & && 0 \leq \gamma_n \leq \bar{Q}_n, \quad n \in \mathcal{F}, \end{aligned} \tag{1}$$

over γ_n^t for $n \in \mathcal{F}$ and $t = 0, \dots, T-1$. Here, Δt equals 1 minute, the length of the interval. The first constraint enforces HEA n to fulfill its charging obligations over its dwell-time. The second constraint imposes restrictions on charging rates allowed by the airplane battery and the power electronics. Charging power of a battery is often measured in terms of its C-rate. A power capacity of 1C for a specific battery implies that it requires one hour to fully charge it up to its capacity. A number x C indicates a power capacity x times that of 1C. We encode a 10C limit in \bar{Q}_n for each flight, given that higher C-rates are deemed unrealistic (per [34]), treating the next flight's energy requirement as the battery capacity. A

²The energy requirement of a flight is upper bounded by the battery capacity. Encoding a C-rate constraint in \bar{Q}_n using that capacity ensures that our charging schedule always respects the physical charging rate constraints.

quadratic function is strictly convex, minimization of which seeks to reduce the aggregate charging rate at each time and its variance across time, within constraints. One can utilize other increasing strictly convex penalization to enforce the same. Our formulation with the quadratic penalty is inspired by valley-filling algorithms in ground electric vehicle charging problems as in [35].

TABLE III: Highest daily peak power demand in several airports with naive and smart charging.

Airpt.	# of flights being replaced	Highest peak (MW) under naive charging	Shaved peak (MW) under smart charging
ATL	212,205	194.5	98.5
ORD	158,991	138.7	63.5
DFW	103,177	94.3	38.9
SFO	66,737	60.3	25.2
IAD	35,085	55.1	27.1
SAN	20,876	30.3	14.6

Table III records the results from six airports for the days with the highest daily peaks from HEA charging under the naive uniform charging scheme using MF=25%, BSED=700 Wh/kg. The optimization is solved in Python with a Gurobi solver. The results illustrate that daily peaks can substantially reduce through smart charging.

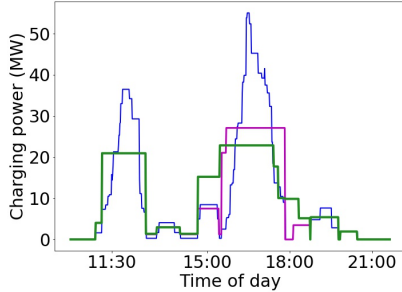


Fig. 5: Charging profiles with naive uniform charging rate (—), smart charging (—), and smart charging with marginally altered flight schedules (—) at IAD on Dec 6, 2018.

Marginal alterations in flight schedules can further shave peak power demands. Even a latitude of 30-minutes in the flight departure times of a few flights can reduce daily peaks. For example, the highest daily peak of 55.1 MW for IAD under uniform charging reduces to 27.1 MW under smart charging; even manual marginal flight schedule alteration reduces it further to 22.9 MW. That is, manually altering the schedules of a few flights within 30 minutes yielded a reduction in peak power from 27.1 MW to 22.9 MW. Figure 5 plots the charging profiles under the three schemes.

IV. CONGESTION MANAGEMENT WITH HEA

Our preliminary experiments in the previous section reveal that charging of HEA and scheduling of aircraft must account for the burdens of grid infrastructure upgrades required to support HEA. In this section, we study congestion management protocols with HEA. We begin in Section IV-A by presenting a flight rescheduling problem that jointly minimizes alterations to schedules submitted by the airlines and charging profiles of

HEA to abide by airport operational constraints and charging capacity considerations. Then in Section IV-B, we discuss mechanisms for airport congestion control, where airlines propose schedules that include HEA aircraft routes, and airports utilize the flight rescheduling and charging algorithm to check for feasibility and suggest altered schedules. If the output schedule differs too much from an airline's proposed schedule, the airline must update its proposal, based on business needs and operational considerations across multiple airports. One can consider a variety of update mechanisms; we focus on two that allow airlines to alter their aircraft routes operated by HEA to conventional aircraft. Altering the usual minimization of *displacements* of output schedules from requested schedules of flights to respect declared capacities at an airport, we tackle charging considerations of HEA within airline fleets. Specifically, we build on [19] and [26] among others, and extend with HEA charging constraints.

A. Flight Rescheduling with Smart HEA Charging Algorithm

Consider the rescheduling and charging problem over T intervals, denoted $0, \dots, T-1$. Let \mathcal{S} describe the flight scheduling requests (both arrivals and departures) within this horizon; each request is for departure or arrival of a flight in one among T time intervals. Encode the request in

$$A_i^t := \begin{cases} 1, & \text{if request } i \text{ must be fulfilled at/after period } t, \\ 0, & \text{otherwise} \end{cases} \quad (2)$$

for $t = 0, \dots, T-1$ and $i \in \mathcal{S}$. The binary sequence $(A_i^0, \dots, A_i^{T-1})$ assumes the form $(1, \dots, 1, 0, \dots, 0)$, where the position of the last one indicates the time interval to execute request i . Akin to A_i^t , define Y_i^t for $i \in \mathcal{S}$ and $t = 0, \dots, T-1$ that encodes the allocation decisions instead of requests. That is,

$$Y_i^t := \begin{cases} 1, & \text{if allocation } i \text{ is fulfilled at/after period } t, \\ 0, & \text{otherwise} \end{cases} \quad (3)$$

for $t = 0, \dots, T-1$ and $i \in \mathcal{S}$. For meaningful allocations, we must have

$$Y_i^t \geq Y_i^{t+1}, \quad Y_i^1 = 1, \quad Y_i^t \in \{0, 1\} \quad (4)$$

for all $i \in \mathcal{S}$ and $t = 0, \dots, T-1$. These constraints imply that $(Y_i^0, \dots, Y_i^{T-1})$ becomes a sequence of the form $(1, \dots, 1, 0, \dots, 0)$, where the position of the last one describes the time interval allocated to request i .³ Declared capacity of an airport is described by the number \bar{R} of arrivals and departures that an airport can handle within a horizon of L time intervals. This number encodes operational constraints that arise due to limited number of runways, gate management schemes and available staff, among others. Thus, we impose the constraint

$$\sum_{i \in \mathcal{S}} \sum_{\tau=t}^{\min\{t+L, T-1\}} (Y_i^\tau - Y_i^{\tau+1}) \leq \bar{R} \quad (5)$$

³One can alternately formulate the problem with variables $\tilde{Y}_i^t \in \{0, 1\}$ that indicate whether allocation i is fulfilled exactly at period t . While a formulation with such variables does not introduce conceptual difficulties, the notation becomes more cumbersome; we circumvent that by adopting the formulation in [25]

for each $t = 0, \dots, T-1$. In general, many airports consider different capacities over different time horizons; we use a representative \bar{R} for simplicity.

Let \mathcal{C} describe the set of pairs (j, j') of requests from \mathcal{S} , where j is an arrival request and j' is the corresponding departure request. Then, we impose a lower bound $\underline{W}_{j,j'}$ on connecting times for flights at the airport as

$$\sum_{t=0}^{T-1} (Y_{j'}^t - Y_j^t) \geq \underline{W}_{j,j'} \quad (6)$$

for all $(j, j') \in \mathcal{C}$, given that the intervals t over which $Y_{j'}^t = 1$ and $Y_j^t = 0$ are exactly those for which the airplane is at the airport.

Let \mathcal{C}^H denote the subset of \mathcal{C} with requests of HEA. For $(j, j') \in \mathcal{C}^H$, let $E_{j,j'}$ denote the total energy demand for the aircraft whose arrival/departure requests are indexed by j, j' . Let $\gamma_{j,j'}^t$ denote the charging rate during time interval t for the battery of the aircraft that is identified by the requests j, j' . The energy needs of that aircraft is enforced via

$$\sum_{t=0}^{T-1} (Y_{j'}^t - Y_j^t) \gamma_{j,j'}^t \Delta t = E_{j,j'}, \quad \gamma_{j,j'}^t \geq 0. \quad (7)$$

Here, Δt is the length of each time interval and hence, $\gamma_{j,j'}^t \Delta t$ is the energy delivered to a connecting airplane over time interval t . Such a constraint is enforced for all $(j, j') \in \mathcal{C}^H$. In addition, we impose two sets of constraints on the power delivered to the HEA. First, the aggregate power for charging all HEA across the airport is constrained by \bar{P} , the capacity defined by the grid infrastructure at the airport, as

$$\sum_{(j,j') \in \mathcal{C}^H} (Y_{j'}^t - Y_j^t) \gamma_{j,j'}^t \leq \bar{P} \quad (8)$$

for each $t = 0, \dots, T-1$. Second, we enforce that charging rates for each individual battery does not exceed 10C. Specifically, we impose an upper bound $\bar{Q}_{j,j'}$ on the charging rate of the form

$$\gamma_{j,j'}^t \leq \bar{Q}_{j,j'} \quad (9)$$

for each $(j, j') \in \mathcal{C}^H$ and $t = 0, \dots, T-1$. Similar to that in (1), we use the energy requirement of the flight as a proxy for the battery capacity to compute $\bar{Q}_{j,j'}$.

For a request $i \in \mathcal{S}$, define its *displacement* as the positive (respectively, negative) difference X_i^+ (respectively, X_i^-) between the time interval allocated and the time interval requested, i.e.,

$$X_i^+ := \sum_{t=0}^{T-1} (1 - A_i^t) Y_i^t, \quad X_i^- := \sum_{t=0}^{T-1} A_i^t (1 - Y_i^t). \quad (10)$$

With this notation, we present the flight rescheduling and charging problem as the following optimization problem.⁴

$$\begin{aligned} \text{minimize} \quad & \sum_{i \in \mathcal{S}} (X_i^+ + X_i^-) + w_0 \max_{i \in \mathcal{S}} \max \{X_i^+, X_i^-\} \\ & + w \sum_{t=0}^{T-1} \left(\sum_{(j,j') \in \mathcal{C}^H} \gamma_{j,j'}^t \right)^2, \\ \text{subject to} \quad & (4) \text{ for } i \in \mathcal{S}, t = 0, \dots, T-1, \\ & (5) \text{ for } t = 0, \dots, T-1, \\ & (6) \text{ for } (j, j') \in \mathcal{C}, \\ & (7), (8) \text{ for } (j, j') \in \mathcal{C}^H, \\ & (9) \text{ for } (j, j') \in \mathcal{C}^H, t = 0, \dots, T-1, \\ & (10) \text{ for } i \in \mathcal{S} \end{aligned} \quad (11)$$

over the variables Y , γ and X . The objective function is a weighted combination of three terms. The first term is the maximum displacement. The second summand equals the total displacement over all flights. The third summand is a penalty that is designed in a way that minimizing it favors flat aggregate charging profiles of HEA *across* flights, similar in spirit to the smart charging problem in (1). The positive constant w controls the trade-off between minimizing displacements and peak-shaving in charging the HEA. Assigning a low weight w amounts to prioritizing the minimization of displacements of movement requests at the expense of higher peak powers required to charge the HEA. Note that while \bar{P} in (8) imposes a hard constraint on the total power drawn by HEA at the airport, the third term in the objective function with $w > 0$ seeks to additionally flatten the demand profile within these limits. \bar{P} encodes capacity constraints of the supporting grid infrastructure at the airport. Operating within these limits, peak shaving is crucial to minimize energy costs of airports. Sharp peaks in power demands are typically met with expensive generators, the added expense of which are levied on consumers through peak demand charges. These charges are calculated based on the maximum power usage, instead of the net energy consumption, and are common elements of electric utility rate structures across the US. Interaction between electric transit buses and peak demand charges are recorded in [36]. Given the magnitude of the peak charging power requirements of airports due to HEA charging, electric peak demand charges can be substantial for airports. Airlines paying for such charges will likely pass these costs on to passengers, increasing travel costs. Positive w can aid in flattening the power profile and reducing the peak power below \bar{P} .

The rescheduling and charging problem in (11) is a mixed-integer optimization program with a convex quadratic objective function and a mix of linear and bilinear constraints. Notice that all bilinear forms in the constraints such as those in (7) and (8) are products of two variables, one among which is binary, and the other is a continuous variable. Constraints that involve linear combinations of bilinear forms can be

⁴In the interest of concreteness, we design (11) with a specific objective function. One can formulate the same with additional considerations for both transportation and charging.

replaced by equivalent linear constraints as follows. Consider a bilinear term of the form $\alpha_B \alpha_R$, where $\alpha_R \in [\underline{\alpha}_R, \bar{\alpha}_R]$ and $\alpha_B \in \{0, 1\}$. Then, replace $\alpha_B \alpha_R$ in the constraint with another continuous variable α , and add the linear constraints,

$$\begin{aligned} \underline{\alpha}_R \alpha_B &\leq \alpha \leq \bar{\alpha}_R \alpha_B, \\ \underline{\alpha}_R(1 - \alpha_B) &\leq \alpha_R - \alpha \leq \bar{\alpha}_R(1 - \alpha_B). \end{aligned} \quad (12)$$

Upon repeating this exercise with each bilinear form in the constraint, we obtain a set of linear constraints that can be shown to be equivalent to the original bilinear constraint. Thus, products between binary and continuous variables in such constraints can be handled equivalently as mixed-integer linear constraints. With said reformulations, (11) can be solved as a mixed-integer quadratic program. Popular solvers such as Gurobi implement the above reformulation internally.⁵

B. Alteration of Proposed Schedules Based on Outputs of Rescheduling Algorithm

Consider the setting where multiple airlines propose their schedules (including the reflecting of certain aircraft routes with HEA), but the rescheduling and charging algorithm used by the airport outputs a modified schedule that is quite different from the proposed one. We assume that the current schedules at the airports reflect airlines' scheduling preferences truthfully. Scheduling requests are made based on customer demand, competitors' schedules, and historical performance data of said schedules, among other factors. Consequently, airlines may find large modifications to their proposed schedules unacceptable. Therefore, one needs mechanisms for airlines to alter their proposed schedules and iterate the process with the airport.

Formally, let \mathcal{A} denote the set of airlines. For $a \in \mathcal{A}$, let \mathcal{S}_a define the set of scheduling requests from airline a . Further, let \mathcal{C}_a define the set of pairs (j, j') of requests from \mathcal{S}_a , where j is an arrival request and j' is the corresponding departure request. Define the subset \mathcal{C}_a^H of \mathcal{C}_a that contains the requests from HEA. Consider the case where all airlines $a \in \mathcal{A}$ have submitted their scheduling requests \mathcal{S}_a to the airport. Then, the airport runs the rescheduling and charging problem in (11). If the maximum among the optimal displacements X_i^+ and X_i^- from (11) exceed a pre-set limit such as 10 or 15 minutes, some among the airlines may find it unacceptable and must alter their proposed schedules and/or aircraft routes operated via HEA. That is, each airline a must then resubmit \mathcal{S}_a and \mathcal{C}_a^H for the airport to adjust the schedules. Also note that in general literature, small schedule displacements of less than 15 minutes have been assumed to not affect the airline's competitive position significantly relative to their competitors [37], [38].

While each airline a should have the flexibility to resubmit \mathcal{S}_a and \mathcal{C}_a^H , in this paper, we consider a restricted re-submission policy—each airline is asked to *switch* one HEA operated flight path in their requested schedule to conventional (reduce $|\mathcal{C}_a^H|$ by one for each a), while the requested schedule \mathcal{S}_a is maintained the same. Some remarks about our considered

re-submission policy are in order. First, we acknowledge that an airline's inability to alter the proposed schedule is limiting; however, this simple readjustment of HEA operated flight paths is enough to illustrate the impact of HEA charging needs on the output schedules from (11) in our experiments—the key focus of this paper. Second, the reduction of the number of HEA operated flight paths by one for each airline is motivated to maintain equity across airlines. We acknowledge that in the growing literature on tactical mechanisms for congestion management, a myriad ways exist to be equitable amongst airlines for rescheduling, e.g., by accounting for the number of passengers affected, size of airlines, etc.; see [38], [39] for examples. Our policy choice is simple and again, serves to illustrate the effect of HEA-related considerations in the schedule readjustment process. Third, airline a must consider a variety of factors in choosing which particular HEA flight path should be switched to a conventional aircraft. Such considerations include scheduling/charging constraints at other airports, HEA-handling costs that can vary over time, availability of different aircraft, etc. Again, we adopt a simple approach and pick the flight path in \mathcal{C}_a^H that has the highest *uniform charging rate requirement*. Such a choice is heuristic, and is guided by the intuition that a connection whose next flight on the route requires a high uniform charging rate over the dwell time at the airport imposes heavy burdens on the charging infrastructure, accommodating which likely causes large displacements of flights. Thus, its removal will likely reduce maximum displacements. This heuristic capitalizes on the impact of HEA charging on displacements.

Overall, our readjustment of schedules proceeds as follows. When the output schedule from (11) is deemed unacceptable by an airline, they each offer to reduce the number of HEA-operated flight paths by one, chosen based on ranking said flight paths based on their uniform charging requirements. Then, the airport reruns (11) with modified \mathcal{C}_a^H 's, and the process continues. The algorithm is visualized in Figure 6 on the left. If the proposed schedules with all HEA switched to conventional aircraft results in acceptable displacements for all airlines, then this iterative procedure must converge.

The mechanism described above requires each airline to resubmit a scheduling request. One might surmise that the airport can itself reduce HEA-operated flight path requests centrally. For the sake of comparison, we consider an additional mechanism (see the right of Figure 6), where the airport ranks all HEA-operated flight paths from the collection of airlines and reduces that set by one, based on the path that has the highest uniform charging rate across the airport. It then re-solves (11) and this cycle continues, till the displacements are deemed acceptable by the airlines.⁶ Again, if the proposed schedules with all HEA switched to conventional aircraft yield acceptable displacements for all airlines, then this cycle must converge. We remark that such a centralized procedure for the readjustment of schedules will take away the autonomy of the airlines to choose their aircraft-type (and more generally, their schedules), and hence, may prove challenging to implement.

⁵See <https://www.gurobi.com/events/products-of-variables-in-mixed-integer-programming/>.

⁶One can include a constraint of the form $\max\{X_i^+, X_i^-\} \leq \bar{X}$ in (11) to encode a hard constraint on maximum displacements that airlines might tolerate.

We conclude this section with a remark about our modeling choices to compute the rescheduling and charging decisions. We recognize that our formulation in (11) and the negotiation mechanisms in Figure 6 can be made much more comprehensive, allowing for extensions to capture IATA guidelines as in [25], airline equity and interests as in [38], [39], and connecting passenger flows as in [40]. While we aim to pursue these directions in future research, our focus in this paper is to illustrate the need for jointly modeling scheduling and charging decisions associated with HEA reflecting, using HEA concepts that are deemed viable in 2030-2050. Our case study, presented next, is dedicated to this task.

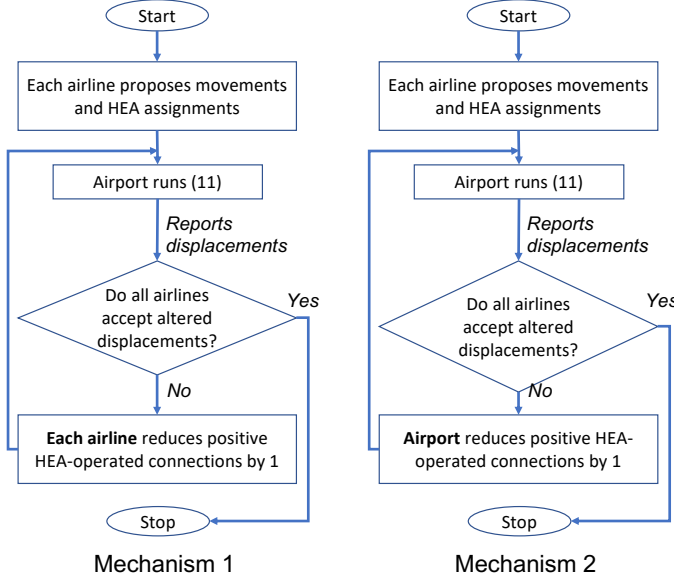


Fig. 6: Two heuristic mechanisms to alter HEA-operated connections.

V. CASE STUDY OF FLIGHT RESCHEDULING DUE TO HEA FOR THE JFK AIRPORT

We now conduct a representative case study for domestic flight operations at the JFK airport based on flight schedules on December 27, 2018. Specifically, we utilize the schedules of domestic flights from the BTS database for the JFK airport as the requested movements over the peak hours of 10:00-16:00, considering each time interval to be 2 minutes in length. Per the BTS dataset, there were 215 movements during this time window. We consider the actual movements as the scheduling requests. A more representative study requires data of the actual scheduling requests from airlines for which our use of the realized schedules only serve as a proxy. Among the requesting aircraft, 32 of them with arriving /departure request pairs can be switched to the hybrid electric option, based on the selection criterion described in Section II with BSED of 700 Wh/kg and MF of 25%—conservative parameter choice for attainable BSED and mid-range of expected MF in the 2030-2050 time-frame. According to [41], JFK supports around 90 arrivals and departures per hour. For our first set of experiments, we consider a capacity of $\bar{R} = 45$ over $L = 30$ slots for domestic flights, roughly allocating half the total capacity at JFK to domestic flights, per the share of domestic

flights among all flights served at JFK (see [42]). We encode a minimum connecting time of 30 minutes in \underline{W} for all aircraft.

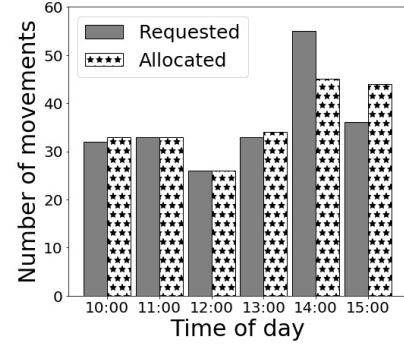


Fig. 7: Requested and allocated movements per hour at JFK airport on 12/27/2018; allocation decisions are based on the benchmark experiment that does not consider HEA charging.

First, we run the optimization problem in (11) without accounting for charging considerations. That is, we drop the constraints (7), (8) and (9) in (11) and set $w = 0, w_0 = 1$. In effect, we run an optimization problem only over the displacement variables Y, X . The outcome of this experiment serves as a benchmark to compare the subsequent results with charging considerations. Figure 7 illustrates that the resulting allocation decisions exhibit some displacements from requested schedules. Such displacements are inevitable, given that the peak hourly slot request exceeds our assumed airport's considered capacity of $\bar{R} = 45$. With the resulting rescheduling decisions, we construct a charging profile for HEA that will result from a uniform charging rate over their dwell times at the JFK airport. Charging HEA at a constant power level over the resulting allocations then yields a peak power demand of 35.9 MW.

Next, we consider an upper bound of $\bar{P} = 20$ MW on the total power drawn by HEA at the JFK airport. This capacity is far less than the peak power of 35.9 MW obtained under a uniform charging schedule added to the rescheduling problem that ignores charging considerations. Encoding a realistic 10C battery charging rate in \bar{Q} 's, we run (11) with two different choices of w . With $w_0 = 1, w = 0$, we obtain a charging profile whose peak power is 20.0 MW, that equals the airport's charging capacity. That is, even without explicitly seeking to flatten the aggregate charging profile across HEA via the objective, the optimization problem finds a slot allocation and charging schedule that respects charging capacity limits at the airport, enforced via (8). Even when the peak power respects said limits, it is useful to flatten the charging profile and reduce peak powers to avoid large peak demand charges. Upon choosing $w_0 = 1, w = 1/\bar{P}^2$, we obtain a charging profile whose peak power is 14.6 MW, that is even less than that obtained with $w = 0$. Thus, positive w aids in peak shaving.⁸ To see this, we keep $w_0 = 1$ and reduce the value of w to $1e^{-13}$, the resulting peak power rises to 20.0 MW. This

⁷By positive displacement, we mean non-zero $X_i^+ + X_i^-$, i.e., we omit the cases with no displacement and $X_i^+ + X_i^- = 0$.

⁸In general, it can happen that peak power drawn with $w = 0$ and $w > 0$ become \bar{P} , where positive w will flatten the resulting charging profile further than with zero w , albeit with coinciding peaks.

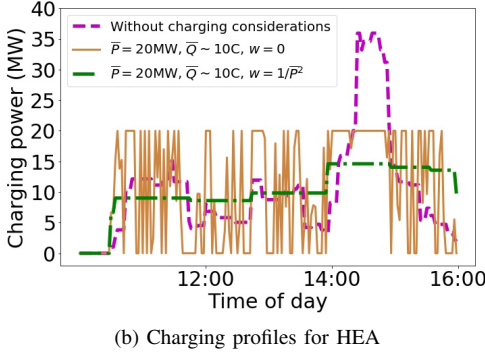
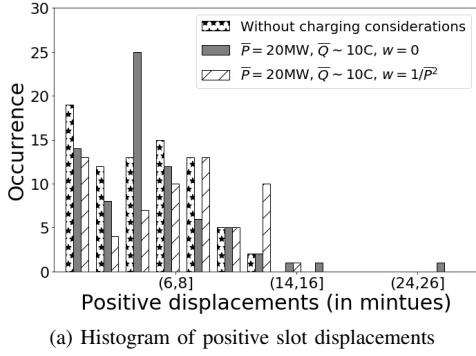


Fig. 8: Positive displacements⁷ and charging profiles for three different parameter sets: (1) Rescheduling decisions without charging constraint under uniform charging (2) $\bar{P} = 20$ MW, $w = 0$, $\bar{Q} \sim 10C$ and (3) $\bar{P} = 20$ MW, $w = 1/\bar{P}^2$, $\bar{Q} \sim 10C$. For all experiments, \bar{R} is held constant at 45.

is due to the fact that we impose less stringent requirement on the peak shaving performance. The displacements from these experiments are visualized in Figure 8a and the charging profiles are plotted in Figure 8b. These figures demonstrate that charging considerations impact not only the charging schedules but they also affect the resulting flight schedules. In the same vein, changing the upper bound on the battery charging rate \bar{Q} impacts both displacement decisions and charging profiles. Figures 9a and 9b capture this sentiment through an experiment with $\bar{P} = 20$ MW, $w_0 = 1$, $w = 1/\bar{P}^2$, $\bar{R} = 45$, where \bar{Q} encodes two different battery charging limits of 5C and 10C.

As one might expect, expanding the airport capacity \bar{R} to accommodate 50 flight movements instead of 45 movements per hour should reduce the extent of rescheduling. Indeed, aggregate displacements reduce non-linearly from 502 minutes with $\bar{R} = 45$ to 206 minutes with $\bar{R} = 50$. Figure 10a confirms that the overall distribution of displacements skews leftward from this expanded runway capacity. This experiment utilizes $\bar{P} = 20$ MW, $w = 1/\bar{P}^2$, $w_0 = 1$ and \bar{Q} encodes a charging rate upper bound of 10C. Change in runway capacity from $\bar{R} = 45$ to $\bar{R} = 50$ not only alters the flight schedules, but it also changes the resulting charging profiles (see Figure 10b). The peak power changes from 14.6 to 16.0 MW. To explain this increase, note that an expanded airport capacity allows more arrivals and departures in each time interval. As the throughput during peak hours increases, the aggregate power demand from the HEA during these peak hours concomitantly

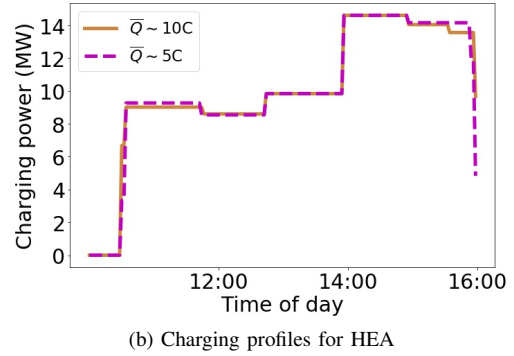
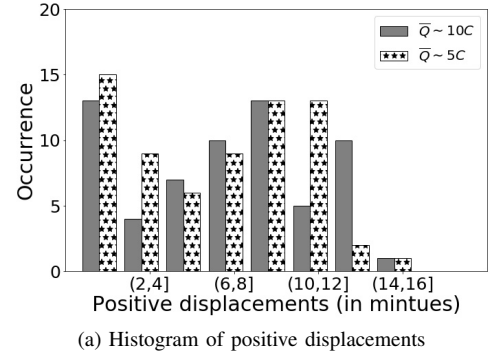


Fig. 9: Positive displacements and charging profiles with $\bar{P} = 20$ MW, $w_0 = 1$, $w = 1/\bar{P}^2$, $\bar{R} = 45$ and two different choices for battery charging capacities: $\bar{Q} \sim 10C$ and $\bar{Q} \sim 5C$.

increases. This experiment illustrates that airport's capacities to handle transportation throughput not only impact flight schedules but also significantly affect the charging profiles and their peaks.

The above experiments demonstrate that constraints on airport capacities as well as those imposed on HEA charging affect both flight schedules and charging profiles with adoption of HEA in commercial aviation. One cannot simply tackle flight scheduling and HEA charging separately; these two questions are inextricably linked. We remark that while we only report the results from JFK, the framework is general and can be applied to any airport.

Finally, we consider the question of how proposed schedules are altered when the outputs of (11) cause longer displacements than what an airline deems acceptable (assume the maximal acceptable displacement is 10 minutes in this experiment for all airlines). To test the two mechanisms for altering proposed schedules, we first generate a schedule by running (11) with a declared capacity of $\bar{R} = 50$, $\bar{P} = 14$ MW, $\bar{Q} \sim 5C$ and $w_0 = 1$, $w = 1/\bar{P}^2$. The solution features a peak charging power of 13.8 MW with the maximal displacement of 14 minutes.

Based on such modified schedule, we now consider the two schemes as summarized in Figure 6 to switch HEA-operated connections to conventional aircraft. In the first scheme, each of the 8 airlines drops one HEA-operated connection, by switching those HEA-operated routes to conventional aircraft that require the maximum uniform charging rate among their movements. As a result, their switches convert 8 HEA-operated routes to conventional. After a single iteration, the

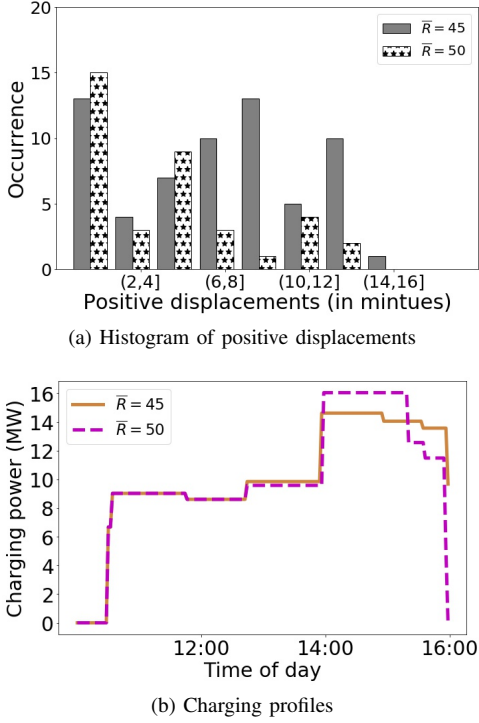


Fig. 10: Positive displacements and charging profiles for two different airport capacities ($\bar{R} = 45$ and 50) with $P = 20$ MW, $w_0 = 1$, $w = 1/\bar{P}^2$ and $\bar{Q} \sim 10C$.

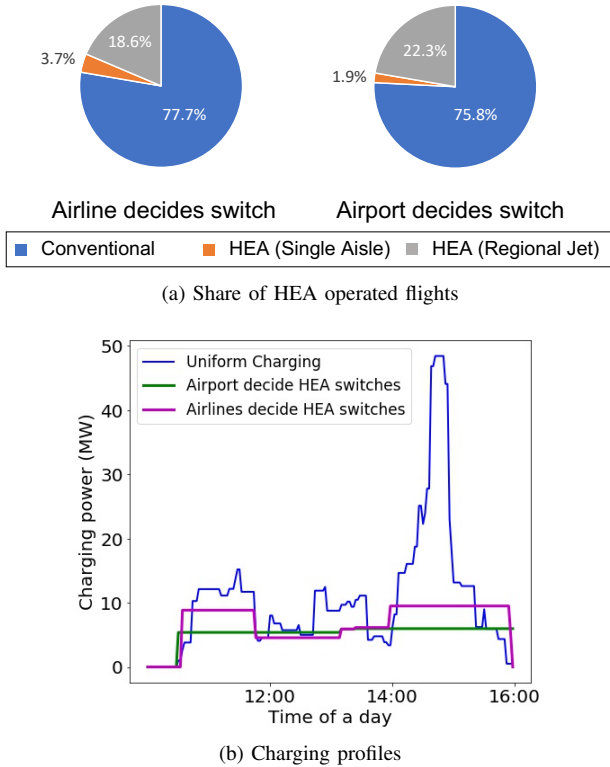


Fig. 11: Comparison of (a) the share of HEA-operated aircraft routes under two different ways to switch such routes/paths to conventional aircraft and (b) charging profiles.

maximum displacement drops from 14 minutes to 8 minutes, making the schedules acceptable to all airlines. In the second mechanism, the airport chooses to switch the single flight path with maximum uniform charging rate among all HEA-operated connections to conventional. Our implementation needs six iterations to reduce the maximum displacement from 14 minutes to 10 minutes. Figure 11a portrays the difference in the proportions of HEA-operated routes. While we consider limited flexibility in the rescheduling process (only allow airlines/airport to switch HEA-operated flight paths to conventional), our result underscores the importance of HEA operations in congestion management. Viewed differently, details of congestion management will likely play a vital role in HEA use.

We remark that the rescheduling and charging problem in (11) is solved in Python with Gurobi [43] version 9.0.2 on a MacBook Pro with Apple M1 pro chip. While the computational time varies (it generally takes longer to solve the problem with tighter constraints), the longer run-times clock around 950 seconds. Gurobi's branch-and-bound algorithm for mixed-integer quadratic programming produces a certifiably globally optimal solution in each run.

VI. CONCLUSIONS AND FUTURE DIRECTIONS

HEA technology is maturing fast. They are projected to become viable for commercial aviation over the next few decades. While their overall energy needs at a national scale had been estimated before, we took a much more nuanced view of airport operations with HEA in this paper. Specifically, we provided a framework to gauge the energy needs of operating a specific aircraft's route with plausible hybrid electric options. This calculation allowed us to estimate the substantial increase in energy demands at major US airports with likely technology growth scenarios. Future technology growth patterns are inherently uncertain, and as a result, our projections of energy requirements bear the burden of that uncertainty. Given the variety of possible technology growth (BSDE/MF combinations), our work provides an estimated range of possible energy capacities required at airports for HEA adoption. We showed through various examples that one must carefully design the charging profile of HEA at airports to reduce peak power demands. Smart management of HEA charging profiles and slight alterations of flight schedules can help to significantly reduce peak power demands at airports. Such reductions can lighten the burdens of required grid infrastructure upgrades and allow airports to avoid peak electric demand charges. Building on this observation, we then proposed a flight rescheduling and charging algorithm that seeks to both minimize displacements of requested movements and flatten aggregate charging profiles. We illustrated our proposed formulation through a case study for JFK airport. The key insight from our analysis is that adoption of HEA within airline fleets will require coordination between flight scheduling and HEA charging. Scheduling and charging cannot be solved separately. While one can choose not to enforce flight rescheduling protocols at the cost of increased delays; by contrast, constraints imposed by the charging infrastructure cannot be frequently violated without seriously damaging the

infrastructure. And coordination of scheduling and charging must be done *across* airlines. Our results illustrate that the specifics of implementation, e.g., who decides HEA-operated flight paths, can substantially alter HEA usage, in turn affecting long-term HEA adoption by airline carriers.

Our rescheduling algorithm with HEA charging is designed for a single airport. Such a framework can be extended in future work to jointly schedule flights and charge HEA across several airports. That framework will allow us to relax the requirement that each airport must fulfill the charging needs of all its outgoing flights. Rather, one can charge HEA at only a few airports that upgrade their grid infrastructure. We do not anticipate conceptual difficulties in formulating such a problem. However, solving such an optimization problem at scale will invariably require careful algorithm design, especially when solved over a long time horizon such as 6 months. Note that our rescheduling and charging algorithm is meant as a planning tool that solves the problem prior to the date the flights are operated. Real-time contingencies such as weather-related variations in runway capacities, unexpected equipment malfunction and crew shortages at airports inevitably require modifications of such plans. We plan to enhance our model to include tactical recourse decisions that adapt to said contingencies, possibly optimizing charging decisions with access to local stochastic solar power generation at an airport. In this paper, we have not explicitly modeled the costs of HEA charging. In future work, we aim to study the design of contracts among electric utilities, airports and airlines to pay for powering HEA. Such a study will allow us to estimate how HEA adoption will impact flight ticket prices as such costs trickle down to passengers.

APPENDIX

Table I: Battery energy usage b_0 in Wh per passenger-mile

Type	MF (%)	BSED (Wh/kg)				
		500	700	1000	1250	1500
Boeing 737-700	12.5	26.5	26.3	25.7	25.4	25.2
	25	57.3	55.5	54.0	53.2	52.6
	50	-	119.8	115.1	112.8	111.2
ERJ-175	12.5	31.1	30.7	30.4	30.2	30.0
	25	64.8	63.6	62.6	62.1	61.6
	50	-	133.3	130.6	129.1	127.9

Table II: Maximum range of HEA in miles

Type	MF (%)	BSED (Wh/kg)				
		500	700	1000	1250	1500
Boeing 737-700	12.5	1110.9	1466.2	1876.8	2141.3	2357.5
	25	558.9	836.1	1193.7	1452.4	1680.1
	50	-	376.1	637.1	842.9	1038.4
ERJ-175	12.5	683.1	914.2	1170.7	1339.7	1476.6
	25	305.9	484.1	714.1	877.45	1020.1
	50	-	170.2	331.2	458.8	579.6

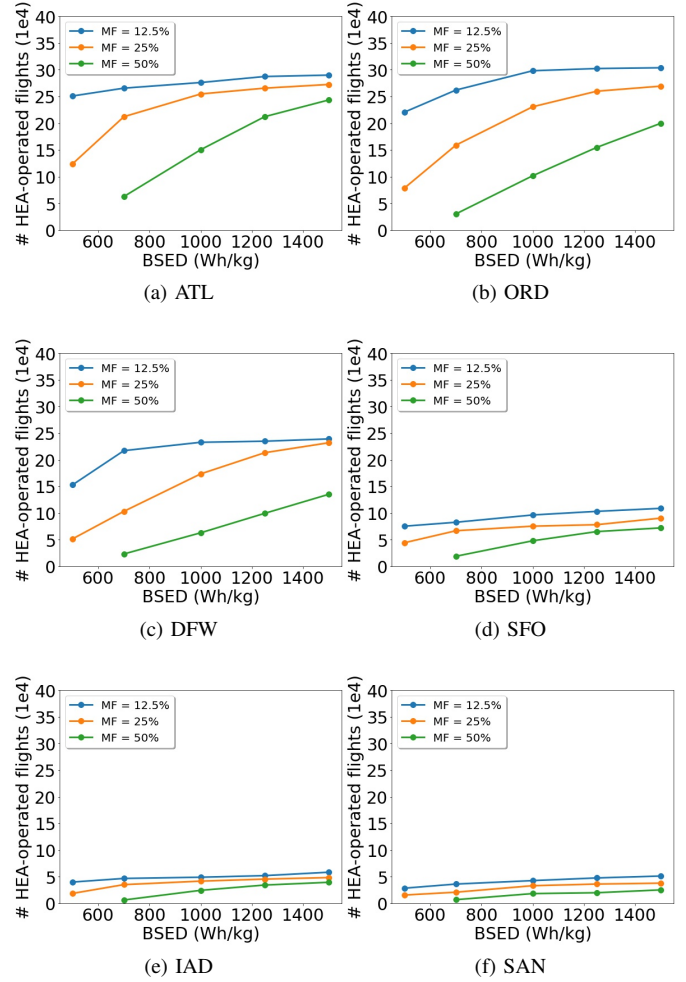


Fig. 12: Number of flights that are switched to HEA under various BSED/MF combinations.

Table III: Number of flight paths from the various airports in 2018, that were operated by a regional jet (RJ) or single aisle (SA) aircraft in the BTS dataset.

Airport	# flights served by RJ/SA
ATL	289,951
ORD	304,651
DFW	239,156
SFO	132,321
IAD	61,455
SAN	56,729

REFERENCES

- [1] Air Transport Action Group, “Air Transport Action Group facts and figures,” 2020. [Online]. Available: <https://www.atag.org/component/factfigures/>
- [2] International Civil Aviation Organization, “Forecasts of scheduled passenger and freight traffic,” 2018. [Online]. Available: <https://www.icao.int/sustainability/pages/eap-fp-forecast-scheduled-passenger-traffic.aspx>
- [3] V. Grewe, A. Gangoli Rao, T. Grönstedt, C. Xisto, F. Linke, J. Melkert, J. Middel, B. Ohlenforst, S. Blakey, S. Christie *et al.*, “Evaluating the climate impact of aviation emission scenarios towards the paris agreement including covid-19 effects,” *Nature Communications*, vol. 12, no. 1, pp. 1–10, 2021.
- [4] National Academies of Sciences Engineering and Medicine, *Commercial aircraft propulsion and energy systems research: reducing global carbon emissions*. National Academies Press, 2016.

- [5] D. Hyde, R. Berz, S. Carter, J. Li, A. Mitchell, R. Riedel, and M. Saposnik, "Target True Zero: Delivering the Infrastructure for Battery and Hydrogen-Powered Flight," World Economic Forum and McKinsey & Company, Tech. Rep., 2023.
- [6] C. Lents, L. Hardin, J. Rheau, and L. Kohlman, "Parallel hybrid gas-electric geared turbofan engine conceptual design and benefits analysis," *52nd AIAA/SAE/ASEE Joint Propulsion Conference, 2016*, pp. 1–13, 2016.
- [7] P. Bertrand, T. Spierling, and C. E. Lents, "Parallel hybrid propulsion system for a regional turboprop: Conceptual design and benefits analysis," p. 4466, 2019.
- [8] J. C. Gladin, D. Trawick, D. Mavris, M. Armstrong, D. Bevis, and K. Klein, "Fundamentals of parallel hybrid turbofan mission analysis with application to the electrically variable engine," *2018 AIAA/IEEE Electric Aircraft Technologies Symposium, EATS 2018*, pp. 1–16, 2018.
- [9] A. W. Schäfer, S. R. Barrett, K. Doyme, L. M. Dray, A. R. Gnadt, R. Self, A. O'Sullivan, A. P. Synodinos, and A. J. Torija, "Technological, economic and environmental prospects of all-electric aircraft," *Nature Energy*, vol. 4, no. 2, pp. 160–166, 2019.
- [10] G. E. Wroblewski and P. J. Ansell, "Mission Analysis and Emissions for Conventional and Hybrid-Electric Commercial Transport Aircraft," *Journal of Aircraft*, no. January, pp. 1–14, 2019.
- [11] K. Zografos, M. Madas, and K. Androustopoulos, "Increasing airport capacity utilisation through optimum slot scheduling: review of current developments and identification of future needs," *Journal of Scheduling*, vol. 20, no. 1, pp. 3–24, 2017.
- [12] IATA, *Slot Administration*, 2021. [Online]. Available: https://www.faa.gov/about/office_org/headquarters_offices/ato/service_units/systemops/perf_analysis/slot_administration/slot_administration_schedule_facilitation/level-3-airports
- [13] A. R. Gnadt, R. L. Speth, J. S. Sabnis, and S. R. Barrett, "Technical and environmental assessment of all-electric 180-passenger commercial aircraft," *Progress in Aerospace Sciences*, vol. 105, pp. 1–30, 2019.
- [14] M. K. Bradley and C. K. Droney, "Subsonic ultra green aircraft research: Phase I," 2011.
- [15] —, "Subsonic ultra green aircraft research: Phases II," 2015.
- [16] C. Pernet, C. Gologan, P. C. Vratny, A. Seitz, O. Schmitz, A. T. Isikveren, and M. Hornung, "Methodology for Sizing and Performance Assessment of Hybrid Energy Aircraft," *Journal of Aircraft*, vol. 52, no. 1, pp. 341–352, 2014.
- [17] J. Delhay and P. Rostek, "Hybrid Electric Propulsion Europe-Japan Symposium Electrical Technologies for the Aviation of the Future," *Europe-Japan Symposium Electrical Technologies for the Aviation of the Future*, no. March, 2015.
- [18] C. Friedrich and P. Robertson, "Hybrid-Electric Propulsion for Aircraft," *Journal of Aircraft*, vol. 52, no. 1, pp. 176–189, 2014.
- [19] N. Pyrgiotis and A. Odoni, "On the impact of scheduling limits: A case study at Newark Liberty International airport," *Transportation Science*, vol. 50, no. 1, pp. 150–165, 2016.
- [20] NERA Economic Consulting, *Study to assess the effects of different slot allocation schemes*. Report, European Commission, DG TREN, London, 2004.
- [21] A. Czerny, P. Forsyth, D. Gillen, and H. Niemeier, *Airport Slots: International Experiences and Options for Reform*. Ashgate Publishing, Farnham, UK, 2008.
- [22] L. Corolli, G. Lulli, and L. Ntamo, "The time slot allocation problem under uncertain capacity," *Transportation Research Part C: Emerging Technologies*, vol. 46, pp. 16–29, 2014.
- [23] U. Benlic, "Heuristic search for allocation of slots at network level," *Transportation Research Part C: Emerging Technologies*, vol. 86, pp. 488–509, 2018.
- [24] A. Jacquillat and A. R. Odoni, "A roadmap toward airport demand and capacity management," *Transportation Research Part A: Policy and Practice*, vol. 114, pp. 168–185, 2018.
- [25] N. A. Ribeiro, A. Jacquillat, A. P. Antunes, A. R. Odoni, and J. P. Pita, "An optimization approach for airport slot allocation under IATA guidelines," *Transportation Research Part B: Methodological*, vol. 112, pp. 132–156, 2018.
- [26] N. A. Ribeiro, A. Jacquillat, and A. P. Antunes, "A large-scale neighborhood search approach to airport slot allocation," *Transportation Science*, vol. 53, no. 6, pp. 1772–1797, 2019.
- [27] Federal Aviation Administration, "Cost of delay estimates," 2020, Accessed: 2021-08-16. [Online]. Available: https://www.faa.gov/data_research/aviation_data_statistics/media/cost_delay_estimates.pdf
- [28] E. Veldman and R. A. Verzijlbergh, "Distribution grid impacts of smart electric vehicle charging from different perspectives," *IEEE Transactions on Smart Grid*, vol. 6, no. 1, pp. 333–342, 2014.
- [29] S. I. Spencer, Z. Fu, E. Apostolaki-Iosifidou, and T. E. Lipman, "Evaluating smart charging strategies using real-world data from optimized plugin electric vehicles," *Transportation Research Part D: Transport and Environment*, vol. 100, p. 103023, 2021.
- [30] J. R. Pillai and B. Bak-Jensen, "Impacts of electric vehicle loads on power distribution systems," in *2010 IEEE Vehicle Power and Propulsion Conference*. IEEE, 2010, pp. 1–6.
- [31] J. García-Villalobos, I. Zamora, J. I. San Martín, F. J. Asensio, and V. Aperribay, "Plug-in electric vehicles in electric distribution networks: A review of smart charging approaches," *Renewable and Sustainable Energy Reviews*, vol. 38, pp. 717–731, 2014.
- [32] US Department of Transportation's Bureau of Transportation Statistics (BTS), "Airline on-time performance data," 2018. [Online]. Available: https://www.transtats.bts.gov/Fields.asp?gnoyr_VQ=FGK
- [33] —, *US Air Carrier Traffic Statistics through June 2020*, 2020. [Online]. Available: <https://www.transtats.bts.gov/TRAFFIC/>
- [34] Battery University, "BU-401a: Fast and Ultra-fast Chargers," 2021, Accessed: 2021-08-16. [Online]. Available: <https://batteryuniversity.com/article/bu-401a-fast-and-ultra-fast-chargers>
- [35] L. Gan, U. Topcu, and S. H. Low, "Optimal decentralized protocol for electric vehicle charging," *IEEE Transactions on Power Systems*, vol. 28, no. 2, pp. 940–951, 2012.
- [36] J.-B. Gallo, T. Bloch-Rubin, and J. Tomić, "Peak demand charges and electric transit buses," *US Department of Transportation, Tech. Rep.*, 2014.
- [37] S. Lan, J.-P. Clarke, and C. Barnhart, "Planning for robust airline operations: Optimizing aircraft routings and flight departure times to minimize passenger disruptions," *Transportation Science*, vol. 40, pp. 15–28, 2006.
- [38] A. Jacquillat and V. Vaze, "Interairline equity in airport scheduling interventions," *Transportation Science*, vol. 52, no. 4, pp. 941–964, 2018.
- [39] J. Fairbrother, K. G. Zografos, and K. D. Glazebrook, "A slot-scheduling mechanism at congested airports that incorporates efficiency, fairness, and airline preferences," *Transportation Science*, vol. 54, no. 1, pp. 115–138, 2020.
- [40] S. Birolini, A. Jacquillat, P. Schmedeman, and N. Ribeiro, "Passenger-centric slot allocation at schedule-coordinated airports," *Transportation Science*, vol. 57, no. 1, pp. 4–26, 2023.
- [41] Federal Aviation Administration, *John F. Kennedy International (New York) (JFK) Airport Capacity Profile*, 2014. [Online]. Available: https://www.faa.gov/airports/planning_capacity/profiles/media/JFK-Airport-Capacity-Profile-2014.pdf
- [42] The Port Authority of NY and NJ, *The Port Authority Aviation Department's 2018 Annual Traffic Report*, 2018. [Online]. Available: <https://www.panynj.gov/content/dam/airports/statistics/statistics-general-info/annual-atr/ATR2018.pdf>
- [43] G. Optimization *et al.*, "Gurobi optimizer reference manual, 2020," URL <http://www.gurobi.com>, vol. 12, 2012.